Interference in wave-front-division-based spectrometers illuminated with ultrafast pulses of light

L. Grave de Peralta[a)]
Department of Physics, Texas Tech University, Lubbock, Texas 79409, USA

(Received 19 September 2008; accepted 21 November 2008; published online 13 January 2009)

Visually appealing simulations of the ultrafast response of an integrated-optics spectrometer reveal how interference occurs inside of the device and before the light arrives to the external measurement instrument. The device was especially designed for having no more than one pulse at a time in the common path of the spectrometer. Simulations are in excellent agreement with recent experiments involving arrayed waveguide grating pulse shapers. © *2009 American Institute of Physics*.
[DOI: 10.1063/1.3062150]

I. INTRODUCTION

Wave-front-division-based (grating-based) spectrometers are well established instruments with a large variety of applications.[1] These instruments spectrally decompose the electromagnetic radiation injected in the input, resulting in light with different frequencies coming out of distinct outputs of the device.[2] The underlying physical principle behind the spectrometer capabilities is the occurrence of multiple slit interference between light traversing the instrument through a multitude of different paths.[2] Moreover, here interference supposes superposition of electromagnetic fields. When a wave-front-division-based spectrometer is illuminated with a coherent source of continuous wave light, numerous beams defined by the grating superposes in the common path of the interferometer.[2] However, when the spectrometer is illuminated with a coherent source of pulsed light, short pulses of light traverse the instrument through a multitude of different paths.[3–5] If the spectral width of the illumination source is smaller than the free spectral range (FSR) of the spectrometer, the pulses overlap in the common path of the interferometer.[3,4] This results in a single elongated pulse at the interferometer outputs.[3,4] Consequently, narrower output spectra than the spectrum of the input pulse are observed at each output channel of the device.[3,4] That is, grating-based spectrometers can be used to measure the spectral composition of pulsed light having a spectral width smaller than the FSR of the instrument.

Wave-front-division-based spectrometers have been used for sliding a supercontinuum, which is generated by a pulsed light source having a spectral width much larger than the FSR of the instrument.[6,7] Similar conditions occur in direct space to time pulse shapers based on integrated-optics arrayed waveguide grating devices.[8,9] In these cases, pulses do not overlap at all in the common path of the spectrometer.[5] Nevertheless, the spectrometers continue delivering their basic functionality: the capability to spectrally decompose the electromagnetic radiation injected in the input, resulting in light with different frequencies coming out of distinct outputs of the device. Two different explanations have been given to this useful property of the grating based spectrometers. A somewhat disseminated but incorrect justification states that the superposition responsible for the multiple slit interference occurs outside the instrument, for instance, due to the stretching of the pulses in optical filters externally added to the spectrometer.[3,10] The correct explanation states that a pulse can be described as a superposition of monochromatic components;[11] these monochromatic components are very long, thus, before and after the arrival of a pulse such elongated waves do exist, and the superposition of them results in the observed multiple slit interference.[5,12] Perhaps motivated by the mathematics involved, sometimes the correct explanation is somehow considered unphysical but mathematically correct. While the dispersion ability of spectrometers have been exploited in numerous applications involving pulses of arbitrary short duration[6–9] and this topic has been previously addressed in the literature of physics,[3,5,10,12] it appears to be an interesting feature of spectrometers that may still not be widely appreciated by seasoned physicists and engineers outside of the reduced circle of ultrafast optics experts.

This work presents a simple but visually compelling approach for simulating the propagation of ultrafast pulses of light inside of a specially designed integrated-optic spectrometer with a FSR smaller than the spectral width of the pulsed light source of illumination. Recently, the temporal and spectral output responses of such device were experimentally measured and analytically described.[5,9] However, this work provides for the first time a detailed simulation of the temporal, spatial, and spectral evolution of the pulses inside of a wave-front-division-based spectrometer. The simulations described here reveal how the pulses travel one by one through the slab region of the device, which is the only region inside of the device where paths of different pulses intercept each other. Each pulse arrives to the output extreme of the slab before the next pulse appears on its input extreme. Nevertheless, well-defined interference maxima are formed at the output extreme of the slab. A careful analysis of the simulation results establishes that distinct interference maxima corresponds to different frequencies, which is in excellent agreement with the experimental observation that light with different frequencies come out of distinct output

[a)]Electronic addresses: luis.grave-de-peralta@ttu.edu and luisgrave@hotmail.com.

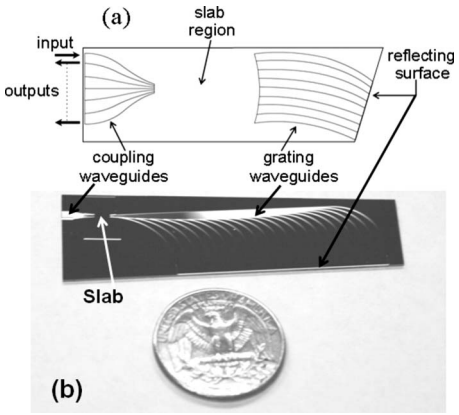

FIG. 1. Schematics (a) and photography (b) of the integrated-optics generalized spectrometer simulated in this work.

channels of the device.[5] The formation of interference maxima in the output slab extreme demonstrates that interference occurs *inside* the spectrometer even when pulses that travel through different paths in the device do not overlap. A straightforward consequence of this observation is discussed in this work: the dispersing ability of spectrometers extends to pulses of arbitrarily short duration as long as the spectral components, corresponding to pulses following distinct optical paths, overlap coherently in the common path of the spectrometer inside of the instrument.

The paper is organized as follows. In Sec. II, a description of the simulated integrated-optic spectrometer is presented. The experimental characterization of the simulated device and additional details about device fabrication are available elsewhere.[4,5] The simulation approach is explained in Sec. III and the simulated results are presented and discussed in Sec. IV. Finally, in Sec. V the conclusions of this work are given.

II. DESCRIPTION OF THE SIMULATED DEVICE

Figure 1 shows a schematic presentation and a photograph of the integrated-optic generalized spectrometer simulated in this work. The device consists of an input-output coupler, a slab region with a length of $f=3$ mm, an arrayed waveguide grating with 21 waveguides, and a reflecting surface. High reflectivity at the reflecting surface is assured by the deposition of a Cr–Au film. The waveguides forming the grating have a constant length increment of $\Delta L=2$ mm. The waveguides of the grating are separated by a distance of $d=20$ μm at the slab extreme and grow rapidly up to more than 25 μm elsewhere. This prevents any light coupling between them. The input-output structure contains one input and six output waveguides, with all waveguides placed perpendicular to the coupler-slab interface. The integrated-optic spectrometer was carefully designed to operate in the following way: when a single incident pulse is injected to the integrated-optic spectrometer through an optical fiber, the pulse diffracts out of the input waveguide. After propagation through the slab region, the pulse illuminates the grating, launching a pulse replica in each waveguide of the grating. The pulse replicas have the same spectrum as the input pulse but lower intensity. After returning from the reflecting surface, each pulse replica diffracts out of a waveguide of the grating and, after propagating back through the slab region, illuminates the input-output coupler, launching an output pulse in each output waveguide. As a result, when the device is illuminated with a single input pulse, the temporal response at each output waveguide is a burst of pulses.

The device was designed to operate under continuous light illumination at a center wavelength of $\lambda_0=1.56$ μm given by the following expression:[13]

$$\lambda_0 = \frac{2n\Delta L}{m}, \tag{1}$$

where $m=3876$ is the grating order and n is the effective refractive index in the waveguides. A design FSR of 50 GHz and a frequency shift of $\Delta\nu_{sh}=25$ GHz between spectra collected at consecutive output waveguides, separated at the slab extreme by a distance of $D=82.1$ μm, were determined by the following expressions:[8,13]

$$\mathrm{FSR} = \frac{c/n}{2\Delta L}, \tag{2}$$

$$\Delta\nu_{sh} \approx \frac{cDd}{2\lambda_0 f\Delta L}, \tag{3}$$

where c is the speed of the light in vacuum. When the integrated-optic spectrometer is illuminated using a pulsed source with a time-limited spectrum having a spectral bandwidth, $\Delta\xi \gg \mathrm{FSR}$ and repetition rate $R \ll \Delta\xi$, the temporal output response of the device is a burst of pulses per incident pulse of light.[5,9] The time separation between consecutive pulses in a burst, $\Delta\tau=1/\mathrm{FSR}$ (Refs. 5, 8, and 9) is much longer than the width of the pulses in the burst $\Delta\tau_p \sim 1/\Delta\xi$ but much shorter than the duration of each burst $\Delta\tau_b \sim N\Delta\tau$, where N is the number of waveguides in the grating. In addition, if the time separation between consecutive input pulses $\Delta\tau_s \sim 1/R$ is larger than $\Delta\tau_b$, the temporal response of the device is a sequence of well-defined bursts of pulses.[9] In these conditions, the arrayed waveguide grating of the device acts as a series of delay lines, where each pulse in the output burst can be associated with a specific waveguide of the grating. Consequently, by correctly choosing the device's parameters, the designer of the integrated-optic generalized spectrometer could guarantee, for instance, that the first pulse to be observed in an output burst must have passed through the shortest waveguide of the grating, or that there is no temporal and spatial overlap between pulse replicas at any moment inside of the device. These conditions were achieved experimentally by using a mode-locked laser with a spectral bandwidth of ~ 7 nm centered at $\lambda_0=1.56$ μm, which emits 0.5 ps pulses with a repetition rate of 50 MHz.[5] The spatial extent of the 0.5 ps pulse replicas in silica glass is ~ 104 μm and the round trip pulse replica-to-pulse replica separation is 4 mm. This is 1 mm longer than the length of the slab region. Therefore, in accordance to the device design, the output pulses related with a pulse replica were already traveling through the output waveguides while the next pulse replica was still traversing the grating. Consequently, in the reported experiments there was never more than one pulse replica at a

time in the slab region, which is the only place inside of the integrated optics spectrometer where superposition of pulse replicas could occur. The spectral and temporal output responses of the fabricated device were measured and theoretically explained using a Fourier optics approach.[5] The spectrum at a single output waveguide consisted of numerous narrow peaks separated by $\Delta\nu \sim 50$ GHz. This is in excellent agreement with the device FSR design value. The intensity autocorrelation trace exhibited a train of pulses with the pulse-to-pulse separation of $\Delta\tau = 1/\Delta\nu \sim 20$ ps, as expected from the time delay imposed by the length increment between consecutive waveguides of the grating. Moreover, the spectral outputs measured at two distinct output waveguides were also compared. In agreement with the design value, a relative shift of ~25 GHz was clearly observed comparing the spectra measured at two consecutive output channels. The observed frequency shift is a characteristic signature of interference in multiple slit experiments. The authors of the experiments therefore concluded that light with different frequencies came out of distinct output waveguides and consequently; it was proposed that interference occurred inside of the integrated-optic spectrometer, without any overlap between pulse replicas, and *before* the light had arrived to the external apparatus used to measure the output spectrum. Strictly speaking, an external optical spectrum analyzer was used in order to know that light with difference frequencies came out of distinct output waveguides of the device. Thus, it may be argued that the interference really occurred in the measurement instrument, where the pulses were elongated and finally overlapped with each other.[3,10] In addition, the Fourier optics approach used to describe the output response of the device is not well suited for obtaining a nonmathematical description of the spatial, temporal, and spectral evolution of the electric fields inside of the slab region of the integrated-optic spectrometer. In order to overcome this issue, a simulation approach capable of providing a compelling visualization of what occurs in the slab region is presented in Sec. III.

III. SIMULATION APPROACH

The only possibility for interference inside of the integrated-optic spectrometer occurs when pulse replicas, coming back from the reflecting surface of the device, travel through the slab region, where paths of different pulse-replicas intercept each other. Basically, what happens after the pulse replicas leave the grating is the well-known phenomenon of diffraction by multiple slits. Following the approach of Wesley,[14,15] a monochromatic double-slit interference pattern can be simulated by the superposition of the monochromatic waves produced by two point sources separated by a distance (d). A straightforward extension of this approach in the case of N slits and pulsed illumination is to consider the superposition of the monochromatic waves produced by a periodical array of N sets of point sources; with the period (d) equal to the distance between consecutive sets in the array and each set formed by $2M+1$ point sources, i.e.,

$$\Psi(x,y,t) = \sum_{i=1}^{N} \sum_{j=-M}^{+M} \Psi_{ij}(x,y,t), \tag{4}$$

where each one of the $N(2M+1)$ monochromatic waves Ψ_{ij} is described by the following expression:[14,15]

$$\Psi_{ij}(x,y,t) = \frac{1}{R_i}\sin\left(\frac{2\pi\nu_j}{c/n}R_i - 2\pi\nu_j t + \varphi_{ij}\right), \tag{5}$$

where R_i is the distance from a given point (x,y) to the center of the ith-slit (set of sources), and ν_j and φ_{ij} are the frequency and initial phase of the wave Ψ_{ij}, respectively. In an arrayed waveguide grating formed by N waveguides with different lengths, the initial phase is given by the following expression:[5]

$$\varphi_{ij} = 2\pi(i-1)m\frac{\nu_j}{\nu_o}, \tag{6}$$

where ν_o $\lambda_0 = c$. Once the function Ψ is known, the magnitude ($S = |\boldsymbol{S}|$) and direction ($\boldsymbol{S}/S$) of the time-averaged energy flux can be computed using the following expression:[14,15]

$$S(x,y,\tau) = -\frac{h\nu_o}{T}\int_{\tau-T/2}^{\tau+T/2} \nabla\Psi\frac{\partial\Psi}{\partial t}dt. \tag{7}$$

T is a convenient time average window and h is the Planck constant [included for making expression (7) dimensionally correct]. The function Ψ is solution of the wave equation:[14]

$$\nabla^2\Psi - \frac{\varepsilon\mu}{c^2}\frac{\partial^2\Psi}{\partial t^2} = 0, \tag{8}$$

where ε and μ are the electric and magnetic permeability of the propagation medium, respectively. The scalar function Ψ is related to the electric $\boldsymbol{E}$ and magnetic $\boldsymbol{H}$ fields through the following expressions:[14,15]

$$\bar{E} = \sqrt{\frac{4\pi\mu h\nu}{c}}\frac{\partial\Psi}{\partial t}\bar{e}, \tag{9}$$

$$\bar{H} = \sqrt{\frac{4\pi h\nu}{\mu}}\bar{e}\times\nabla\Psi, \tag{10}$$

where $\boldsymbol{e}$ is a unit vector perpendicular to the gradient of Ψ and defining the direction of $\boldsymbol{E}$. The simulations shown in Sec. III were obtained using the exact analytical expressions (4)–(6) with parameters corresponding to the integrated-optic spectrometer described above and evaluating numerically the integral (7). The remaining part of this section describes the simulation results corresponding to two important limit cases: a multiple-slit illuminated with monochromatic light and a single aperture illuminated with pulsed light.

Figure 2(a) [Fig. 2(b)] shows the magnitude of the time-averaged energy flux corresponding to $N=21$ ($N=3$) slits illuminated with monochromatic light ($\lambda_0 = 1.56$ μm), with a slit separation $d=20$ μm, and a value of $m=3876$. Figures 2(a) and 2(b) display an area of 0.4×3 mm^2 extended from the input extreme to the output extreme of the slab. The origin of coordinates is at the slab extreme of the central waveguide of the grating. $\boldsymbol{S}$ was calculated using expressions (4)–(7) with $M=0$ and $T=\lambda_0/c$. Characteristic multiple-slit

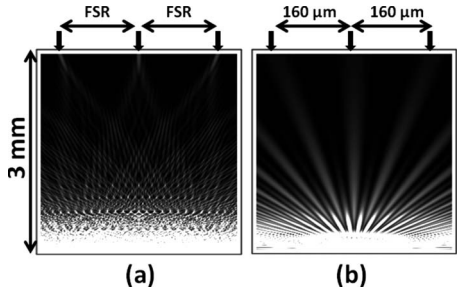

FIG. 2. Magnitude of the time-averaged energy flux corresponding to (a) $N=21$ and (b) $N=3$ slits illuminated with monochromatic light. Characteristic multiple-slit interference maxima (bright regions) and minima (dark regions) are clearly observable. Arrows point to the maxima at the output extreme of the slab.

interference maxima (bright regions) and minima (dark regions) are clearly observable in both figures. The maxima positions at the output extreme of the slab are indicated by the arrows. A free spatial range of $X_{\mathrm{FSR}} \sim 164$ μm is determined from the simulation. This corresponds nicely with the device's design values of FSR=50 GHz and $\Delta\nu=25$ GHz for consecutive output waveguides separated by a distance of $D=82.1$ μm. As expected,[16] the width of the maxima at the output extreme of the slab for $N=21$ [Fig. 2(a)] is smaller than for $N=3$ [Fig. 2(b)]. The focusing effect of the grating in Fig. 2(a) is due to the Pachen's "mounting" geometry (Fig. 1) in the integrated-optic spectrometer.[2,13] It is worth noting that the energy flux distributions shown in Fig. 2 are stationary, i.e., time independent.

Figure 3 shows the instantaneous distribution at $\tau=11$ ps of the magnitude of the time-averaged energy flux corresponding to the case of a single slit simultaneously illuminated by 41 monochromatic sources of light, phase locked by expression (6) with $m=3876$ and with the frequencies given by the following expression:

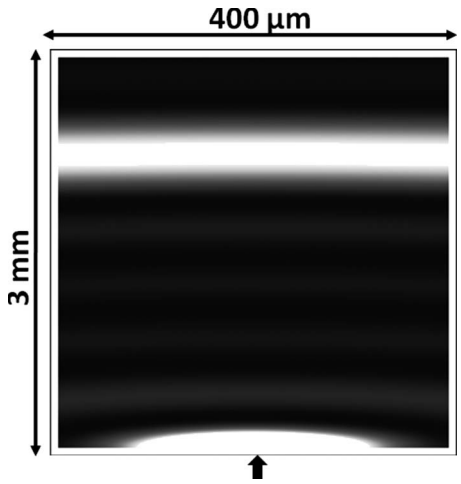

FIG. 3. Instantaneous distribution of the magnitude of the time-averaged energy flux corresponding to a single slit simultaneously illuminated by 41 phase-locked monochromatic sources. The beating between waves with different frequencies results in a pulse of light (horizontal bright band) without transversal structure which propagates through the slab region. The arrow points to the slit.

$$\nu = \nu_o + k\frac{\mathrm{FSR}}{4}, \quad k = 0, \pm 1, \pm 2, \ldots, \pm 20, \tag{11}$$

where FSR=50 GHz. Expressions (6) and (11) correspond to a pulsed illumination source with a spectral bandwidth of $\Delta\xi=10$ FSR=500 GHz, emitting $\Delta\tau_p \sim 1/\Delta\xi=2$ ps pulses with a repetition rate of $R=\mathrm{FSR}/4=12.5$ GHz. $\boldsymbol{S}$ was calculated for $N=1$, $M=20$, $m=3876$, and $T=1/2\nu_o$ in the same area displayed in Fig. 2. Beats[17] between electromagnetic fields with difference frequencies produce the bright horizontal band in Fig. 2. This is a pulse of light without internal structure in the transversal (horizontal) direction. The absence of transversal structure is a characteristic feature of diffraction by a single slit.[2] The longitudinal extension of the pulse in Fig. 3 is ~ 400 μm, in excellent accord with a pulse width of 2 ps. The propagation of the pulse through the slab region was studied by calculating a sequence of 80 frames similar to Fig. 3 (not shown) separated in time by 1 ps. In the first 15 frames a pulse travels from the slit to the slab output. No other pulse propagates through the slab in the 80 ps time period covered by the calculated frames. This is in excellent agreement with a pulsed illumination source with $R=12.5$ GHz which emits a train of pulses separated by $\Delta\tau_s \sim 1/R=80$ ps.

The first limit case illustrated in this section simulates the response of the integrated-optic spectrometer when it is illuminated with monochromatic light. In this case the light beams coming out of distinct waveguides of the grating overlap in the slab region. This results in well-defined interference maxima in the output extreme of the slab (Fig. 2). It is this luminous transversal structure that gives the spectrometer its basic filtering functionality. The second limit case simulates the response of the device when the gold deposited in the reflective surface is removed from all the waveguides of the grating except one. In this case the injected pulse propagates through the slab without any transversal structure (Fig. 3); which makes the modified device just a transmission line without any spectral filtering functionality.

IV. SIMULATION OF THE DEVICE UNDER PULSED ILLUMINATION

Figure 4 shows the instantaneous distribution at $\tau=11$ ps of the magnitude of the time-averaged energy flux corresponding to the case of $N=3$ slits simultaneously illuminated by 41 monochromatic sources of light, phase locked by expression (6) with $m=3876$ and with the frequencies given by expression (11). $\boldsymbol{S}$ was calculated for $N=3$, $M=20$, and $T=1/2\nu_o$ in the same area displayed in Fig. 3. The energy flux distribution displayed in Fig. 4 combines features present in Figs. 2(b) and 3. As in Fig. 3, beats between electromagnetic fields with different frequencies produces the bright horizontal band in Fig. 4. The width of the bright band, $c\Delta\tau_p/n \sim c/n\Delta\xi \sim 400$ μm in both figures, is determined by the spectral width ($\Delta\xi=500$ GHz) of the illumination source defined by expression (11). However, the pulse in Fig. 4 has a transversal structure resembling the interference fringes in Fig. 2(a). As in Fig. 2(b), the bright spots in the pulse in Fig. 4 are formed by constructive interference between monochromatic waves with the same frequency coming out of

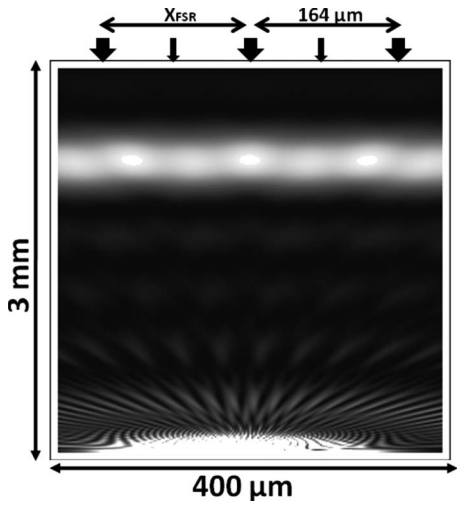

FIG. 4. Instantaneous distribution of the magnitude of the time-averaged energy flux corresponding to $N=3$ slits simultaneously illuminated by 41 phase-locked monochromatic sources. The beating between waves with different frequencies results in a pulse of light (horizontal bright band). The interference between waves with the same frequency coming out of distinct slits produces a transversal structure in the pulse. The pulse propagates through the slab region maintaining its transversal structure.

distinct slits. For instance, three monochromatic waves coming out of the three slits with the design frequency of the device (ν_o) interfere constructively at the center of the transversal structure of the pulse. This also occurs for the ten frequencies in expression (11) differing from ν_o by a multiple of the free spectral range of the device:

$$\nu = \nu_o + k\mathrm{FSR}, \quad k = 0, \pm 1, \pm 2, \ldots, \pm 5. \tag{12}$$

The central spot in the pulse in Fig. 4 is longitudinally (transversally) defined by beating (interference) between monochromatic waves with different (equal) frequencies, which overlap with each other in the device slab region. Consequently, only light with frequencies given by expression (12) arrive to the output waveguide (indicated by the center fat arrow in Fig. 4). A straightforward consequence of this observation is the prediction that the measured spectrum at the central output waveguide of the device should be a periodic set of peaks with a period of $\sim$FSR=50 GHz and centered at ν_o. This simulation prediction correlates with the experimental results reported in Ref. 5. Two other bright spots in the pulse simulation, indicated by fat arrows in Fig. 4, are separated by the free spatial range (X_{FSR}) from the central spot. These two spots are also laterally defined by constructive interference of waves with the frequencies given by expression (12). At both halves of Fig. 4, halfway between two bright spots marked by fat arrows, there is an additional spot indicated by slim arrows in Fig. 4. These maxima are laterally defined by constructive interference between monochromatic waves coming out of the three slits with the following subset of the frequencies defined by expression (11):

$$\nu = \nu_o + k\frac{\mathrm{FSR}}{2}, \quad k = \pm 1, \pm 3, \ldots, \pm 9. \tag{13}$$

Light with the frequencies given by expression (13) is collected at the output waveguides indicated by the slim arrows. Consequently, the simulation predicts that the measured spectrum at the channel adjacent to the central output waveguide should be a periodic set of peaks with a period of $\sim$FSR=50 GHz and shifted by the design value of $\Delta\nu_{\mathrm{sf}}=25$ GHz with respect to the spectrum measured at the central waveguide. This is in excellent agreement with the experimental results reported in Ref. 5.

The time evolution of the magnitude of the energy flux distribution in the slab region was study by calculating 80 frames similar to Fig. 4 (not shown) separated in time by 1 ps. Three pulses with similar transversal structure propagate through the slab within the 80 ps time period covered by the frames. In accordance with the FSR of the device, a time separation between pulses of $\Delta\tau \sim 1/\mathrm{FSR} \sim 20$ ps is determined from the simulation. The time separation between pulses propagating in the slab is determined by the value of $m=3876$ used in the simulation, which is related to the length difference between consecutive waveguides of the grating (ΔL) through expressions (2), (3), and (6). No pulse propagation is observed in the last 20 ps of the simulation. This means that the temporal output response of the device is a burst of 3 pulses per incident pulse of light. The pulsed illumination source has a spectral bandwidth of $\Delta\xi=10$ FSR=500 GHz, emitting $\Delta\tau_p \sim 1/\Delta\xi=2$ ps pulses with a repetition rate of $R=\mathrm{FSR}/4=12.5$ GHz or pulse-to-pulse time separation of $\Delta\tau_s \sim 1/R=80$ ps. The time separation between consecutive pulses propagating through the slab $\Delta\tau=1/\mathrm{FSR}=20$ ps is longer than the width of the pulses in the burst $\Delta\tau_p \sim 1/\Delta\xi=2$ ps but shorter than the duration of each burst $\Delta\tau_b \sim 3\Delta\tau=60$ ps. At any time in the simulation there is at most a single pulse propagating through the slab because it takes $\sim$15 ps to each pulse to traverse the slab region. Individual pulses never overlap inside of the slab region of the device because a pulse leaves the slab before the next pulse enters. In these conditions, the arrayed waveguide grating of the device acts as a series of delay lines where, as shown in Fig. 5, each pulse in the output burst can be associated with a specific waveguide of the grating.

Figure 5 shows a magnified view of the genesis of the pulses that propagate through the slab region of the device. Pictures in Fig. 5(a) [Fig. 5(b)] correspond to the instantaneous distribution of the magnitude of the time-averaged energy flux calculated in an area of 0.08×1 mm^2 (80×100 μm^2) at times $\tau=1$, 21, 41, and 61 ps as described above. Figure 5(b) clearly shows that a pulse enters to the slab region by a different waveguide of the grating at times $\tau=1$, 21, and 41 ps. In contrast, no pulse enters to the slab at $\tau=61$ ps.

The simulation results presented in this section are not exact simulations of the experiments reported in Ref. 5. Aside from the fact that the real device has 21 waveguides in the grating, the illumination source used in Ref. 5 was a mode-locked laser centered at $\lambda_0=1.56$ μm, which emits 0.5 ps pulses with a repetition rate of 50 MHz. In order to simulate this illumination source the following frequencies should be included in the simulation:

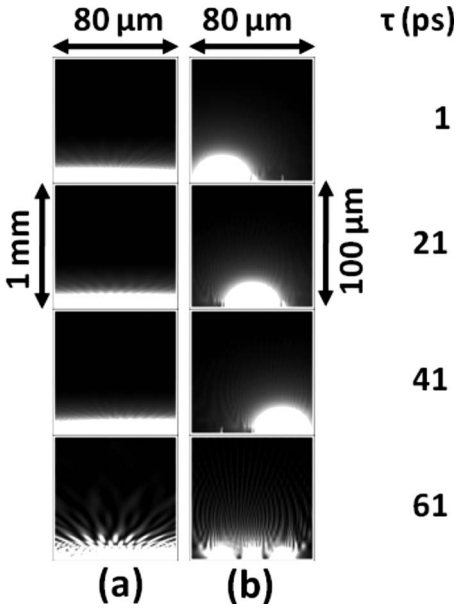

FIG. 5. Instantaneous distribution of the magnitude of the time-averaged energy flux corresponding to $N=3$ slits simultaneously illuminated by 41 phase-locked monochromatic sources and calculated in an area of (a) 0.08×1 mm^2 and (b) 80×100 μm^2. Each pulse enters the slab region by a distinct slit.

$$\nu = \nu_o + k\frac{\mathrm{FSR}}{1000}, \quad k = 0, \pm 1, \pm 2, \ldots, \pm 2 \times 10^4. \quad (14)$$

This large number of frequencies would make the simulation impractical. However, the presented simulations fill in the loopholes existing in the description of the experiments described in Ref. 5. Now it is clear that the observed frequency shift of ~25 GHz between spectra measured at consecutive output waveguides of the device is due to interference occurring inside of the slab region and before the light arrives to the external apparatus used to measure the output spectra. The interference occurs between monochromatic waves with the same frequency coming out of distinct waveguides of the grating. These monochromatic waves overlap in the slab region. At the same time, beating between monochromatic waves with different frequencies results in the formation of pulses. Pulses do not overlap inside of the device. Moreover, at any given time, there is not more than a single pulse propagating in the slab region. The overlapping of pulses is not a necessary condition for the filtering functionality of the spectrometer.

V. CONCLUSIONS

A simple but visually compelling approach for simulating the propagation of ultrafast pulses of light inside of an integrated-optic generalized spectrometer has been presented. Superposition of monochromatic waves produced by a periodical array of N sets of point sources, each set formed by $2M+1$ sources with different frequencies, was used to simulate pulse propagation in the slab region of the device. The simulations presented in this work reveal how the pulses travel one by one through the slab region of the device, which is the only region inside of the device where paths of different pulses intercept each other. It is apparent that in the simulated device, each pulse arrives to the output extreme of the slab before the next pulse appears on its input extreme. Nevertheless, well-defined interference maxima are formed at the output extreme of the slab. A careful analysis of the simulation results establishes that distinct interference maxima correspond to different frequencies, which agrees with the experimental observation that light with different frequencies came out of distinct output channels.[5,9] The formation of interference maxima in the output slab extreme demonstrates that interference occurs inside the generalized spectrometer even when pulses that travel through different paths in the device do not overlap. An important consequence of this observation is that the dispersing ability of spectrometers extends to pulses of arbitrarily short duration as long as the spectral components, corresponding to pulses following distinct optical paths, overlap coherently in the common path of the spectrometer inside of the instrument.

[1] E. G. Loewen and E. Popov, *Diffraction Gratings and Applications* (Dekker, New York, 1997).
[2] M. Born and E. Wolf, *Principles of Optics*, 2nd ed. (Pergamon, New York, 1964).
[3] B. Rubin and R. M. Herman, Am. J. Phys. **49**, 868 (1981).
[4] L. Grave de Peralta, A. A. Bernussi, and H. Temkin, J. Lightwave Technol. **25**, 2410 (2007).
[5] L. Grave de Peralta, A. A. Bernussi, and H. Temkin, IEEE J. Quantum Electron. **43**, 473 (2007).
[6] T. Morioka, K. Uchiyama, S. Susuki, and M. Saruwatari, Electron. Lett. **31**, 1064 (1995).
[7] I. Y. Khrushchev, J. D. Bainbrigde, J. E. A. Whiteway, I. H. White, and R. V. Petty, IEEE Photonics Technol. Lett. **11**, 1659 (1999).
[8] D. E. Leaird and A. M. Weiner, IEEE J. Quantum Electron. **37**, 494 (2001).
[9] D. E. Leaird, S. Shen, A. M. Weiner, A. Sigita, S. Kamei, M. Ishii, and K. Okamoto, IEEE Photonics Technol. Lett. **13**, 221 (2001).
[10] N. H. Abramson, Appl. Opt. **32**, 5986 (1993).
[11] C. Froehly, B. Colombeau, and M. Vampouille, Prog. Opt. **20**, 63 (1983).
[12] S. L. Chin, V. Francois, J. M. Watson, and C. Delisle, Appl. Opt. **31**, 3383 (1992).
[13] K. Okamoto, *Fundamentals of Optical Waveguides* (Academic, New York, 2000).
[14] J. P. Wesley, *Causal Quantum Theory* (Wesley, Blumberg, Germany, 1983).
[15] J. P. Wesley, Found. Phys. **14**, 155 (1984).
[16] A. A. Bernussi, L. Grave de Peralta, S. Frisbie, and H. Temkin, Appl. Phys. Lett. **83**, 1695 (2003).
[17] T. S. Stein and L. G. Dishman, Am. J. Phys. **50**, 136 (1982).